Journal of Environmental Management 289 (2021) 112452

Contents lists available at ScienceDirect

Journal of Environmental Management

journal homepage: http://www.elsevier.com/locate/jenvman

# A novel optical biosensor for in situ and small-scale monitoring of bacterial transport in saturated columns

Wei Tao [a,b,*], Yantao Song [b], Naresh Singhal [b], Cushla McGoverin [c,d], Frédérique Vanholsbeeck [c,d], Simon Swift [e]

[a] School of Chemistry and Environmental Engineering, Sichuan University of Science and Engineering, Zigong, 643000, PR China
[b] Department of Civil and Environmental Engineering, The University of Auckland, Private Bag 92019, Auckland, 1142, New Zealand
[c] The Dodds-Walls Centre for Photonic and Quantum Technologies, The University of Auckland, Private Bag 92019, Auckland, 1142, New Zealand
[d] Department of Physics, The University of Auckland, Private Bag 92019, Auckland, 1142, New Zealand
[e] Department of Molecular Medicine and Pathology, The University of Auckland, Private Bag 92019, Auckland, 1142, New Zealand

ARTICLE INFO

*Keywords:*
Optrode
Bacterial transport
Rhamnolipid surfactant
Fluorescence
Column study

ABSTRACT

*In situ* monitoring techniques can provide new insight into bacterial transport after inoculating exogenous bacteria into contaminated soils for bioremediation. A real-time and non-destructive optical sensor (the optrode) was employed to monitor *in situ* transport of two fluorescently labelled bacteria – Green Fluorescent Protein (Gfp)-labelled, hydrophilic *Pseudomonas putida* and Tomato Fluorescent Protein (td)-labelled, hydrophobic *Rhodococcus erythropolis,* in a saturated sand column with and without rhamnolipid surfactant. *In situ* measurements were made at three sampling ports in the column with the optrode in two sets of column experiments. In Experiment 1, liquid samples were extracted for *ex situ* analyses (plate counts and fluorescence), while in Experiment 2 no liquid samples were extracted. Extracting liquid samples for *ex situ* analyses in Experiment 1 disturbed *in situ* measurements; *in situ* measured bacterial concentrations were lower, or a significant lag in breakthrough occurred relative to *ex situ* measurements. In Experiment 2, the optrode worked well in monitoring bacterial transport, which gave consistent transport parameters at each sampling port. Moreover, the optrode enabled the impact of bacterial hydrophobicity and rhamnolipid surfactant on bacterial transport to be observed. Specifically, hydrophilic *P. putida* was transported faster through the column than hydrophobic *R. erythropolis*; we infer from this result that fewer *P. putida* cells adsorb to sand particles than do *R. erythropolis* cells. The rhamnolipid surfactant enhanced the transport of both hydrophilic and hydrophobic bacteria. These two observations are consistent with Lifshitz–van der Waals forces and acid-base interactions between bacteria and sand.

## 1. Introduction

*In situ* bioremediation has emerged as a potentially cost-effective and environmentally friendly treatment method when compared to *ex situ* bioremediation (Mohan et al., 2006). Inoculating contaminated soil with exogenous bacteria is a common approach to stimulate *in situ* bioremediation by expanding the population of bacteria able to degrade the contaminant. Understanding the transport behaviour of exogenous bacteria is a key aspect to determining the success of this environmental engineering application, because poor penetration of bacteria applied to soil will result in poor bioremediation performance (Li and Logan, 1999; Martin et al., 1996).

The transport behaviour of bacteria within soil is a well-developed area of study (Bai et al., 1997; Brown and Jaffé, 2001; Guo et al., 2021; He et al., 2019). The conventional monitoring method for bacterial transport is *ex situ* measurement where liquid samples are collected from the effluent or a sampling port (Guo et al., 2021; Unc and Goss, 2003; Zhong et al., 2016) and are then analysed by various methods, e.g. total viable counts on agar plates, fluorescence-based microscopy, and flow cytometry (Banning et al., 2002; Maraha et al., 2004). As a result, *ex situ* measurement methods are constrained by factors such as difficulties in monitoring the bacteria attached to soil particles, limited sample size, and the time-consuming process of sampling and analysis (Barbee and Brown, 1986; Di Bonito et al., 2018). The development of *in*

* Corresponding author. School of Chemistry and Environmental Engineering, Sichuan University of Science and Engineering, Zigong, 643000, PR China
*E-mail address:* weitao@suse.edu.cn (W. Tao).

https://doi.org/10.1016/j.jenvman.2021.112452
Received 2 August 2020; Received in revised form 5 March 2021; Accepted 17 March 2021
Available online 1 April 2021

*situ* methods for monitoring bacterial concentration, that are non-destructive, near real-time and cost-effective, has therefore received increasing research focus to allow researchers to monitor the penetration of bacteria into a soil column (Beutel and Henkel, 2011; Dorn et al., 2005; Yolcubal et al., 2000). The use of biosensors that use electrical, thermal or optical signals to detect specific biochemical reactions mediated by isolated enzymes, tissues, organelles or whole cells (McNaught and Wilkinson, 1997), has become well accepted in a number of applications for *in situ* analyses. For example, optical whole-cell biosensors were successful in monitoring the impact of salt stress on the genetic regulation of the quorum sensing networks (Zhang et al., 2018). In a stainless-steel measurement cell that simultaneously received a waste stream solution and maintenance medium, the overall bioluminescent response of an immobilised biosensor (a *Pseudomonas fluorescens* carrying a *nahG:luxCDABE* gene fusion) was found to be proportional to the naphthalene profile (Heitzer et al., 1994). A *nah-lux* reporter constructed in *Pseudomonas putida* RB1353 went a step further, as this bacterium can metabolise naphthalene and salicylate. In a column study, the *in situ* increase in the luminescence response of *Pseudomonas putida* RB1353 was measured using a fibre optic system, and was correlated with the decrease in salicylate and dissolved oxygen concentrations during biodegradation of salicylate (Yolcubal et al., 2000). Later, the fibre optic system successfully captured the growth of the *P. putida* RB1353 biosensor during naphthalene catabolism (Dorn et al., 2005). A fibre-optic spectroscopic probe (optrode) has previously been used to rapidly identify and quantify green and red fluorescently labelled *Pseudomonas*. *putida* NZRM 852, *Escherichia coli* 536, *Escherichia coli* MG165 in a liquid suspension and sand (Hewitt et al., 2012). Optical biosensors offer the possibility of *in situ* analysis because they enable real-time quantification, require no laboratory analysis of liquid samples and allow for non-destructive signal detection, particularly in traditionally light-impenetrable environments (Beutel and Henkel, 2011; Hewitt et al., 2012). As shown by the studies we mentioned above, although much attention has been given to the bacterial transport in substrate environments and optical biosensors have been used to study specific processes involved in bioremediation, almost no information is available in the literature regarding *in situ* monitoring bacterial transport for the purpose of bioremediation. Moreover since bacterial transport monitoring has been mainly based on liquid samples extracted from the system (Unc and Goss, 2003; Zhong et al., 2016) without concurrent *in situ* measurements, the impact of *ex situ* measurements on bacterial transport has not been clarified.

Hence, we investigate the hypothesis that bacterial cells in a column can be quantified by the optrode and that the optrode can be used to monitor bacterial transport *in situ*. We compare the behaviour of bacterial transport between experiments where *ex situ* samples are or are not taken to highlight the benefit of using the optrode for *in situ* monitoring and the impact of *ex situ* measurements on the bacterial transport. The hydrophobicity of bacteria and soil are important factors that can affect the penetration of bacteria (Chen and Strevett, 2001; Zhong et al., 2016), where hydrophobic bacteria have a stronger affinity to soil particles than hydrophilic bacteria (Chen and Zhu, 2004; Huysman and Verstraete, 1993). The addition of surfactants was found to alter the surface hydrophobicity of bacteria and soil (Bai et al., 1997; Chen et al., 2004; Zhong et al., 2016). Therefore, the second research objective is to use *in situ* monitoring by the optrode to investigate the effect of bacterial hydrophobicity on bacterial transport in the presence or absence of surfactant. Two representative fluorescently labelled bacteria, hydrophilic *Pseudomonas putida* KT2442 tagged with green fluorescent protein and hydrophobic *Rhodococcus erythropolis* tagged with Tomato fluorescent protein were used in the study. These two bacterial strains were selected because (1) hydrophobic bacteria have a stronger affinity to soil particles than hydrophilic bacteria (Abu-Zreig et al., 2003; Chen and Zhu, 2005; Gross and Logan, 1995), (2) rhamnolipid surfactant can modify bacterial surface hydrophobicity (Feng et al., 2013), (3) they are commonly found in natural soil environments and (4) have pedigree for PAH degradation (Aitken et al., 1998; Dennis and Zylstra, 2004; Lang et al., 2016; Trzesicka-Mlynarz and Ward, 1995). In this study, the parameters of bacterial transport, Lifshitz-van der Waals and acid-base interaction energy between bacteria and sand particles were studied to understand the behaviour of bacterial transport.

## 2. Materials and methods

### 2.1. Surfactant and bacterial strains

Rhamnolipid (JBR 210, JENEIL ® Biosurfactant Co.), a water solution with 25%, was used as biosurfactant in the model column system. Rhamnolipid is a rhamnose-containing glycolipid surfactant that is primarily produced by *Pseudomonas aeruginosa* and has low toxicity to bacteria (Zhang et al., 1997; Zhao et al., 2011) . A 1000 mg/L rhamnolipid solution was prepared, which is considerably larger than the critical micelle concentration (CMC) of rhamnolipid (40 mg/L) (Clifford et al., 2007; Zhang and Miller, 1994). The prepared rhamnolipid solution was then adjusted to pH ~7 and an ionic strength of 0.01 M to simulate the typical soil environment.

Two pure strains of bacteria were used: hydrophilic Gram negative *P. putida* ATCC 47054 (also known as KT2440) was obtained from the American Type Culture Collection (ATCC) via Cryosite (Australia) and a spontaneous rifampicin-resistant mutation was selected to recreate KT2442 for counter selection (de Lorenzo et al., 1993). The strain was labelled with Gfp using mini-Tn7 transposon system according to Lambertsen et al. (2004) to create *P. putida* KT2442-Gfp. Hydrophobic Gram positive *R. erythropolis* DSM 43066 was obtained from the New Zealand Reference Culture Collection, (ESR, Porirua, New Zealand) and transformed with pTEC27 plasmid DNA encoding the red fluorescent protein tdTomato (pTEC27 is a mycobacterial plasmid containing the red fluorescent protein tdTomato, resistant to hygromycin) (Takaki et al., 2013), using the electroporation protocol previously described by Goude, and Parish (2009) to create *R. erythropolis* (pTEC27). pTEC27 was a gift from Lalita Ramakrishnan (Addgene plasmid # 30182; http://n2t.net/addgene:30182; RRID:Addgene_30182).

### 2.2. Bacterial culture conditions and preparation of column inocula

For the column trials, a colony of *P. putida* KT2442-Gfp was grown overnight in a 100 mL sterile flask with 20 mL of fresh tryptic soy (TS) broth at 28 °C, and constant shaking at 200 rpm. To ensure enough bacteria were prepared for each column experiment, 10 aliquots of overnight culture (2 mL) were taken, and each used to inoculate 200 mL of fresh TS broth in 1000 mL flask. These flasks were incubated overnight at 28 °C. *P. putida* KT2442-Gfp was harvested by centrifugation (8000×*g*, 10 min). *R. erythropolis* (pTEC27) was grown on fresh TS agar plates containing 0.1% of 50 mg/mL hygromycin B and then incubated at 28 °C for 72 h until red colonies formed. Four plates of *R. erythropolis* (pTEC27) were harvested using a moistened cotton swab for each trial to prepare sufficient bacteria. The harvested cells were washed by suspending cells in saline and then centrifuging (8000×*g*, 10 min), this cycle was repeated three times to remove the soluble extracellular polymeric substance. The washed cells were resuspended in 0.01 M NaCl without or with rhamnolipid surfactant at 1000 mg/L (pH~7) for experiments. The bacterial concentration in column inocula and column eluates was determined using a PerkinElmer EnSpire 2300 multilabel plate reader -run with Wallace Envision Manager software. The fluorescence signal of *P. putida* KT2442-Gfp was detected using 485/5 nm excitation and 530/20 nm emission filters; and the fluorescence signal of *R. erythropolis* (pTEC27) was measured by 550/8 nm excitation and 580/10 nm emission filters. Doubling dilutions of culture to 1/1024 dilution, covering $5.0 \times 10^8$–$1.0 \times 10^{11}$ CFU/mL, were prepared in triplicate with and without rhamnolipid surfactant addition. Fluorescence signal was measured from 0.2 mL of the diluted bacterial suspension using the plate reader immediately after dilution and then 10 μl of the suspension was

spread on nutrient agar plates. The CFU were counted the next day and it was assumed that a single bacterium grows into a single colony on the agar plate. For both *P. putida* KT2442-Gfp and *R. erythropolis* (pTEC27), a linear relationship was observed between fluorescence intensity and bacterial concentration (both without and with rhamnolipid addition), with $R^2$ values greater than 0.9597. (Fig S1).

### 2.3. The optrode detection system

#### 2.3.1. The optrode system

The setup of the optrode (Fig. 1) has been described in previous studies (Guo et al., 2017; Hewitt et al., 2012). Measurement of Gfp and Tomato protein fluorescence used laser excitation of 473 nm (blue) and 532 nm (green), respectively; and emission spectra with peaks at 535 and 581 nm for *P. putida* KT2442-Gfp and *R. erythropolis* (pTEC27), respectively, were observed. The fluorescence signal emitted by rhamnolipid when excited at 473 nm is regarded as background and subtracted from the signals. The fluorescence intensity was calculated by integrating across an area around the peak in the emission spectra. The at-sample laser power was measured using a photodiode and adjusted to 7 mW, after a laser stabilization period of 60 min. The fibre core, cladding and coating diameters were 200, 220, and 250 μm, respectively, and the fibre core has a numerical aperture of 0.22. The optrode probes were prepared by fitting a fibre through a 22 g flat-point needle (OD 0.72 mm) and filing it with epoxy to protect the fibre from damage when inserting the probe inside the column, as shown in Fig. S2. The optrode collected fluorescence intensity in liquid media from the collection volume of the fibre i.e., a cone with a base diameter of 200 μm, an angle of 12° and a depth of 900 μm (Hewitt et al., 2012; Tai et al., 2007). Spectra were collected from 400 to 790 nm using an Ocean Optics QE65000 spectrometer. The effect of external factors such as soil particles and rhamnolipid surfactant can be minimized by using signal spectral regions where the background interference is minimal (Hewitt et al., 2012; Tai et al., 2007).

#### 2.3.2. Data collection and analysis

A customised computer data acquisition program was developed using LabVIEW (National Instruments Co) to collect and analyze the optrode fluorescence intensity. Spectral data were collected using a stepped protocol over sequentially doubling integration times: 8, 16, 32, 64, 128, 256, 512, 1024 and 2048 ms. The minimum integration time to achieve a signal-to-noise ratio of 10 was used in subsequent data analyses. Background spectra for each sampling port were recorded before injecting the bacterial suspension into the column. The dark noise and background spectra, matched for integration time, were subtracted from each sample spectrum. The resulting spectrum was normalized to a laser power of 1 mW and an integration time of 1 ms.

#### 2.3.3. Calibration of the optrode fluorescence intensity to bacterial concentration

As it is difficult to gain the direct calibration of the optrode fluorescence intensity and bacterial concentration in the sand column, two sets of batch experiments were conducted to obtain an indirect calibration. Doubling dilutions of a bacterial suspension ($1.0 \times 10^8$–$1.0 \times 10^{11}$ CFU/mL) were prepared in saline in the absence of sand. The first batch experiment consisted of recording optrode fluorescence intensity by dipping the fibre tip into 1.5 mL microtubes of the diluted bacterial suspension and the optrode intensity was plotted against the bacterial concentration (Fig S3). In the second batch experiment, the diluted bacterial suspension was mixed with sand in 1.5 mL microtube using the water to sand ratio (0.234) used inside the column; and the optrode fluorescence intensity of bacteria with sand was collected by submerging the probe in the bacteria-sand system. The optrode intensity with sand was plotted against the optrode intensity obtained without sand (Fig S4). **More details about the optrode signal calibration are provided in the supplementary information**. All samples were prepared in triplicate, and in the absence and presence of rhamnolipid surfactant. Background spectra were collected from six bacteria-free samples: three samples without surfactant and another three samples with surfactant. Therefore, the calibration of the optrode fluorescence intensity to bacterial concentration in the presence of sand can be obtained indirectly through the calibration curves (Fig. S3 and S4).

### 2.4. Column experiments

A cylindrical stainless steel column (6.15 cm inner diameter (ID) × 41 cm length (L)) was designed with three aqueous sampling ports, termed Port 1, Port 2 and Port 3 which are located at 3.0, 15.5 and 30.5 cm from the inlet of the column, respectively (Fig. 1). The sampling port for the optrode probe is positioned opposite to the location of the liquid sampling ports (Fig. 1). For each experiment, the column was uniformly packed with 1852.4 g of sterilized sand with particle size ranging from

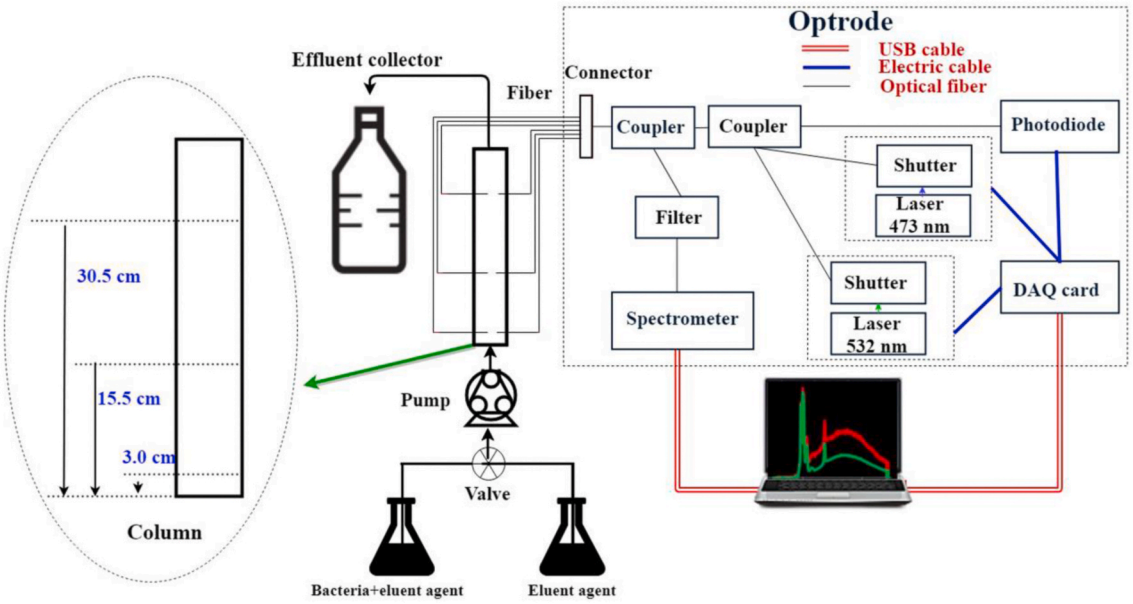


**Fig. 1.** Schematic diagram of the optrode detection system to study bacterial transport in a column model.

0.0625 to 2 mm. The porosity (α) of the packed column was 0.234 as determined from the dry and wet weight of the column. The same sand was used in all column experiments, however, the column was washed with at least 10 L of deionized water until no bacteria or surfactant were detected in the effluent. Comparison of the background spectra collected before all column experiments confirmed the column was free of bacteria after washing.

The background fluorescence signal intensity inside of the column was collected by the optrode after the column had been pre-equilibrated with bacteria-free solutions. To maintain enough cell for *in situ* measurement, approximately $3.5 \times 10^{10}$ CFU/mL of *P. putida* KT2442-Gfp and $8.0 \times 10^{9}$ CFU/mL of and *R. erythropolis* (pTEC27) were pumped into the column for 40 min at a flow rate of 0.432 cm/min, followed by eluting with 700 mL of bacteria-free solution at the same flow rate. The reservoir bacterial suspension was mixed using a magnetic stirrer during each experiment to maintain bacteria in suspension. Two sets of column experiments were conducted to compare the performance of the optrode and *ex situ* measurements in monitoring bacterial transport in the column. Both the optrode and *ex situ* measurements were carried out in the first set of column experiments (Experiment 1). In the second set of column experiments (Experiment 2), the optrode measurements were conducted without sampling for *ex situ* measurements. Results of the optrode presented data of at least 3 runs because the optrode is not able to collect data for all ports in the same run. Results of *ex situ* measurements were averaged data from two runs. The transport of bacteria was expressed as bacterial cell concentration (CFU/mL), which was calculated from fluorescence vs CFU/mL calibration curves in Fig S1, against the pore volumes of eluent liquid agent that were passed through the column. These plots are known as breakthrough curves (BTCs). The pore volumes of eluent liquid agent that passed through the column at time $t$ were calculated using:

$$pore\ volume = \frac{Q \times t}{\pi \times \left(\frac{d}{2}\right) 2 \times L \times a} \tag{1}$$

where $Q$ is pumping rate in mL/min, $t$ is time (min), $d$ is the diameter of the column (6.15 cm), $\alpha$ is the porosity of column and $L$ is the length of the column (41 cm).

### 2.5. The calculation of interaction energy

Because the addition of the surfactant solution did not significantly affect the electrophoretic mobility of the bacteria (Zhong et al., 2016), this study only considered the Lifshitz-van der Waals and acid-base (*LW-AB*) interactions ($\Delta G_{bls}$) between bacteria and sand particles. The Lifshitz-van der Waals ($\Delta G_{bls}^{LW}$) and acid-base energy ($\Delta G_{bls}^{AB}$) can be calculated from the surface tension parameters (Absolom et al., 1983; Busscher et al., 1984; Sharma and Hanumantha Rao, 2002; Van Oss, 1995). Then $\Delta G_{bls}^{LW}$, $\Delta G_{bls}^{AB}$ and $\Delta G_{bls}$ can be described as:

$$\Delta G_{bls}^{LW} = -2 \times \left(\sqrt{\gamma_b^{LW}\gamma_l^{LW}} + \sqrt{\gamma_S^{LW}\gamma_l^{LW}} - \sqrt{\gamma_b^{LW}\gamma_S^{LW}} - \gamma_l^{LW}\right) \tag{2}$$

$$\Delta G_{bls}^{AB} = 2 \times \left(\sqrt{\gamma_1^+}\sqrt{\gamma_b^-} + \sqrt{\gamma_s^-} - \sqrt{\gamma_l^-} + \sqrt{\gamma_1^+}\sqrt{\gamma_b^+} + \sqrt{\gamma_s^+} - \sqrt{\gamma_l^+} - \sqrt{\gamma_b^-\gamma_s^+} + \sqrt{\gamma_b^+\gamma_s^-}\right) \tag{3}$$

$$\Delta G_{bls} = \Delta G_{bls}^{LW} + \Delta G_{bls}^{AB} \tag{4}$$

where the subscript $b$ denotes bacteria, $l$ denotes liquid, and $s$ denotes sand particles.

The three unknown surface free energy components, $\gamma^{LW}$ (*LW* apolar component), $\gamma^-$ (electron donor), $\gamma^+$ (electron acceptor), in Equations (2) and (3) can be determined using the *LW-AB* approach and Yong's equation (Absolom et al., 1983; Busscher et al., 1984; Sharma and Hanumantha Rao, 2002; Van Oss, 1995) based on the contact angle measurement of three diagnostic liquids with known surface tension components. The contact angle measurement for bacteria followed the same method as previously described by Busscher et al. (1984). Briefly, a homogenous bacterial lawn was prepared and the contact angle was measured using a digital goniometer after placing a drop of diagnostic liquid onto the bacteria lawn. Quartz was used because it is the major component of silica sand and offers a uniform surface for estimating the surface hydrophobicity of silica sand. Details of contact angle results are provided in Table S1.

### 2.6. Data analysis

The bacterial concentrations obtained by *ex situ* and *in situ* measurements were compared for equality of means by one-way analysis of variance (ANOVA) with a confidence level of 95% using the statistical program SPSS. To investigate the effect of the liquid sample removal, the proportion of bacteria and liquid withdrawn from the column for *ex situ* measurements was calculated according to the following parameters: the frequency and size of sampling, the number of cells in the liquid sample and the total amount of liquid and bacteria that had been pumped into the column.

To understand the effect of the liquid sampling on the velocity of each sampling port, we assume that the liquid sample came from the top of the sampling port due to gravity which results in the reduction of the velocity at the port located at a higher position. The velocity at a specific port could be expressed as the sum of the pumping velocity and the accumulation of reduction in velocity due to sampling at the ports located at a lower position. Thus the velocity of a specific sampling port at time t could be calculated using Equation (5):

$$q_t = q_0 + \frac{(n - n_t) \times q_s \times t_s}{t} \tag{5}$$

where $q_0$ is the pumping flow rate (0.432 cm/min), $q_s$ is the velocity of the sampling (cm/min), $t_s$ is the time to take each liquid sample (0.167 min). $n$ is the sum of sampling times at the specific sampling port and at ports located at a higher position at time $t$ (min), and $n_t$ is the sum of sampling times at all sampling ports at time $t$ (min).

Thus, velocity caused by sampling ($q_s$) depends on the volume of each liquid sample, sampling time and the properties of the column, which could be expressed as Equation (6):

$$q_S = \frac{V_S}{\pi \times \left(\frac{d}{2}\right)^2 \times a \times t_s} \tag{6}$$

where $V_s$ is the volume of each liquid sample, which is 0.2 mL, $d$ is the inner diameter of the column (6.15 cm), and $\alpha$ is the porosity of column (0.234).

The mathematical model used in this study considered bacterial transport in the column as the result of convection and diffusion of liquid through the silica sand due to the concentration gradient (Chen and Zhu, 2004) as well as any liquid taken out. Bacteria were considered to be transporting through a uniform, one-dimensional, saturated porous media, and in a steady-state flow. Accordingly, the one-dimensional convention-dispersion equation (CDE) is reduced to (Van Genuchten and Alves, 1982):

$$R_d \frac{\partial C}{\partial t} = D \frac{\partial^2 C}{\partial x^2} - v \frac{\partial C}{\partial x} - \mu C + \gamma \tag{7}$$

where $C$ is the bacterial concentration, $R_d$ is retardation coefficient, $D$ is the dispersion coefficient (includes both diffusion and hydrodynamic dispersion), $t$ is the time, $v$ ($LT^{-1}$) is the average velocity inside the column, $x$ is the distance (L), and $\mu$ is the rate constant for the first-order decay ($T^{-1}$), $\gamma$ is the production rate ($T^{-1}$), which is zero as the growth of

bacteria is not considered during column experiment.

The equilibrium equation was solved using CXTFIT 2.0 in STudio of ANalytical MODels (a public domain Windows-based software package) (Parker and Van Genuchten, 1984; Toride et al., 1995) to obtain the parameters of bacterial transport (e.g. $D$, $R_d$, $\mu$ and $R^2$). This approach has been used previously to successfully predict the adsorption and transport of *Escherichia coli* and *Pseudomonas fluorescens* (Chen and Zhu, 2004).

## 3. Results and discussion

### 3.1. Comparison of ex situ and in situ measurements in experiment 1

#### 3.1.1. Comparison of BTCs

BTCs produced by *ex situ* and *in situ* measurements in Experiment 1 were compared, as shown in Figs. 2–5 (**a** and **b**). ANOVA tests suggest the bacterial concentrations observed by these two techniques were significantly different ($P < 0.05$). For *P. putida* KT2442-Gfp, a lower cell concentration was measured by the optrode *in situ* (Fig. 2b) than by plate reader using *ex situ* samples (Fig. 2a), particularly at Ports 2 and 3. The breakthrough point in the BTCs for *P. putida* KT2442 Gfp transport monitored by the optrode was delayed compared to those detected using *ex situ* samples at Port 2 and Port 3 (Fig. 2 a vs. **b** and Fig. 3a vs. **b**). A maximum delay of 0.5 pore volume in the BTCs of *P. putida* KT2442-Gfp in the presence of rhamnolipid surfactant (Fig. 3b) was observed using the optrode. The fitted transport parameters for the *in situ* and *ex situ* measurements at different sampling ports are presented in Table 1. No trend was found in the value of dispersion coefficients between the *in situ* and *ex situ* measurements. However, the values of the retardation coefficient and first-order decay obtained by fitting BTCs collected by the optrode were greater than the values of *ex situ* measurements in all cases (Table 1). The *in situ-ex situ* trend observations for the transport of *P. putida*-Gfp in Figs. 2–3 (**a** vs **b**) were similar for the transport of *R. erythropolis* (pTEC27) (Figs. 4–5 (**a** vs **b**)). These results reveal that the optrode is capable of *in situ* detection of bacterial mobility but the BTCs measured are different from those measured using *ex situ* liquid samples and the plate reader when measurements are recorded simultaneously. To understand the difference between BTCs measured *in situ* by the optrode and *ex situ* measurements in Experiment 1, the next two sections discuss the homogeneity of column and sampling scale of these two techniques.

#### 3.1.2. The homogeneity of column

One possible explanation for the difference between the *in situ* and *ex situ* measurement in Experiment 1 could be heterogeneity within the packed sand column. This possibility was tested by comparing data obtained at horizontal probe depths of 17 mm and 10 mm at the same vertical position within the column. No significant difference was observed between these two data sets ($P > 0.05$); the correlation coefficient between the two datasets was 0.8631 (Fig. S5). These observations indicate that the column was homogeneously packed and probe depth does not contribute to the difference between *ex situ* and *in situ* measurements observed in Experiment 1.

#### 3.1.3. The effect of sampling scale

Sampling scale refers to the effect of sampling volumes when comparing different monitoring devices. Campbell et al. (1999) observed dissimilar transport behaviour when comparing results produced by monitoring methods with different sampling scales. We hypothesized that the sampling scale might lead to different transport behaviour when monitored with *in situ* optrode and *ex situ* plate reader measurements in Experiment 1. The optrode collects the emission spectra in a tiny volume around the optical fibre (approximately 0.009 $mL^3$) (Hewitt et al., 2012; Tai et al., 2007), which can be regarded as a sampling point. Each *ex situ* measurement collects 0.2 mL of the liquid sample from the sampling port, which could represent the average concentration in a relatively large area above the sampling port. *Ex situ* measurements removed 2.7% of the total injected cell mass, and 6.0% of the total injected liquid from the column, respectively. No impact on the velocity was found at Port 1 (0.432 cm/min) when withdrawing *ex situ* samples (Fig. S6). *Ex situ* measurements slightly decreased the averaged velocity at Port 2 and Port 3 (0.423 and 0.420 cm/min, respectively). Therefore, the difference in BTCs obtained by the optrode and *ex situ* measurements in Experiment 1 may be the result of the disturbances in bacterial concentration and flow rate on pore scale, and slight preferential flow through the column, which is only captured by the optrode when these two techniques are simultaneously applied in Experiment 1.

### 3.2. Comparison of in situ measurements in experiment 1 and experiment 2

To eliminate the effect of *ex situ* measurements on the performance of the optrode, the optrode measurement was taken without withdrawing liquid samples from the column in Experiment 2, as shown in Figs. 2–5 (c). BTCs collected by the optrode in Experiment 2 are significant different ($P < 0.05$) to those obtained in Experiment 1, as shown in Figs. 2–5 (b vs. c), The values of first-order decay ($\mu$) obtained by the optrode in Experiment 1 were smaller than those obtained in Experiment 2 (Table 1), the same is true for the retardation coefficients. No consistent trend was found in the value of dispersion coefficients. These findings are consistent with the hypothesis that taking liquid samples affects the bacterial concentration inside the column, meaning that this technique is not adequate for accurate monitoring of bacterial transport in column.

The optrode in Experiment 2 occasionally obtained fluctuating concentrations in the BTCs (e.g. bacterial concentrations were collected by the optrode between 0.2 and 0.5 pore volumes in Fig. 5c), which is likely caused by the shielding of the probe by sand particles. Meanwhile,

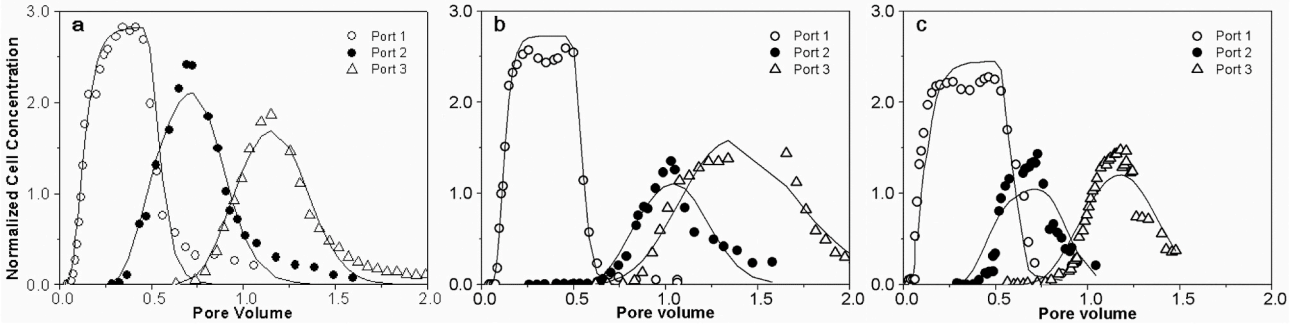


**Fig. 2.** Comparison of the observed and fitted breakthrough curves of *P. putida* KT2442-Gfp in no surfactant obtained by *ex situ* measurements (a), the optrode in Experiment 1 (b) and the optrode in Experiment 2 (c). □, Δ and ⋄ shows the data obtained at Port 1, Port 2 and Port 3, respectively; lines are the fitted data. Cell concentration is normalized by a normalisation factor ($1.0 \times 10^{10}$ CFU/mL).

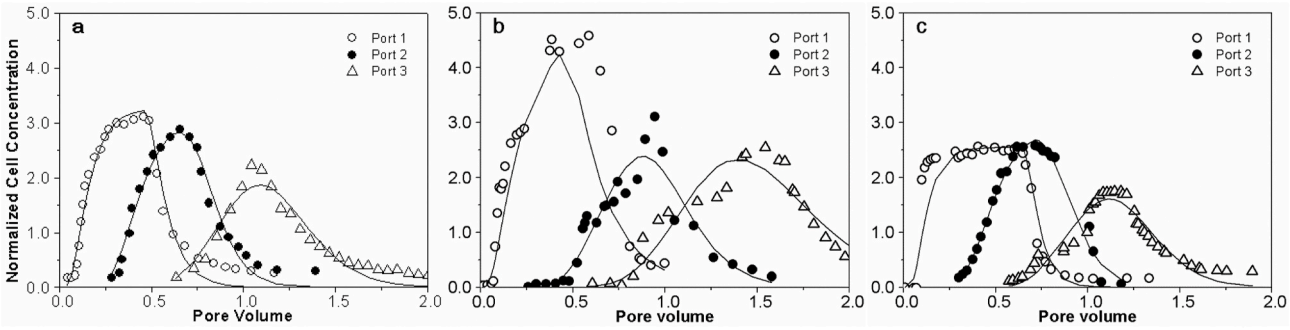


**Fig. 3.** Comparison of the observed and fitted breakthrough curves of *P. putida* KT2442-Gfp in rhamnolipid surfactant obtained by *ex situ* measurements (a), the optrode in Experiment 1 (b) and the optrode in Experiment 2 (c). Symbols and lines are the same as the described in Fig. 2. Cell concentration is normalized by a normalisation factor ($1.0 \times 10^{10}$ CFU/mL).

**Table 1**
Comparison of dispersion coefficients ($D$),retardation coefficient ($R_d$), first-order decay ($\mu$), and coefficient of determination ($R^2$) in BTCs of *P. putida* KT2442-Gfp and *R. erythropolis* (pTEC27) that were monitored by *ex situ* measurements and the optrode.

| Bacteria stains | Experiment condition | | | $D$ (cm$^2$/min) | $R_d$ | $\mu$ (/min) | $R^2$ |
|---|---|---|---|---|---|---|---|
| *P. putida* KT2442-Gfp | **No surfactant** | ***Ex situ* measurement** | Port 1 | 0.12 ± 0.04 | 1.73 ± 0.06 | 0.030 ± 0.005 | 0.952 |
| | | | Port 2 | 0.20 ± 0.04 | 1.30 ± 0.02 | 0.012 ± 0.001 | 0.964 |
| | | | Port 3 | 0.14 ± 0.02 | 1.24 ± 0.01 | 0.008 ± 0.001 | 0.957 |
| | | **Optrode with *ex situ* sampling** | Port 1 | 0.07 ± 0.01 | 1.76 ± 0.03 | 0.1000 ± 0.0030 | 0.986 |
| | | | Port 2 | 0.10 ± 0.04 | 2.27 ± 0.04 | 0.0424 ± 0.0020 | 0.917 |
| | | | Port 3 | 0.42 ± 0.06 | 1.68 ± 0.02 | 0.0088 ± 0.0006 | 0.928 |
| | | **Optrode without *ex situ* sampling** | Port 1 | 0.20 ± 0.06 | 1.30 ± 0.06 | 0.0472 ± 0.0056 | 0.896 |
| | | | Port 2 | 0.15 ± 0.04 | 1.26 ± 0.02 | 0.0338 ± 0.0011 | 0.757 |
| | | | Port 3 | 0.12 ± 0.03 | 1.28 ± 0.01 | 0.0134 ± 0.0005 | 0.892 |
| | **Rhamnolipid** | ***Ex situ* measurement** | Port 1 | 0.23 ± 0.05 | 1.90 ± 0.06 | 0.007 ± 0.004 | 0.960 |
| | | | Port 2 | 0.29 ± 0.05 | 1.09 ± 0.02 | 0.003 ± 0.001 | 0.965 |
| | | | Port 3 | 0.35 ± 0.06 | 1.19 ± 0.02 | 0.004 ± 0.001 | 0.911 |
| | | **Optrode with *ex situ* sampling** | Port 1 | 0.48 ± 0.02 | 2.55 ± 0.23 | 0.0010 ± 0.0100 | 0.795 |
| | | | Port 2 | 0.28 ± 0.05 | 1.87 ± 0.05 | 0.0122 ± 0.0019 | 0.886 |
| | | | Port 3 | 0.50 ± 0.08 | 1.69 ± 0.03 | 0.0004 ± 0.0007 | 0.881 |
| | | **Optrode without *ex situ* sampling** | Port 1 | 0.22 ± 0.04 | 1.20 ± 0.07 | 0.0411 ± 0.0057 | 0.915 |
| | | | Port 2 | 0.26 ± 0.06 | 1.24 ± 0.06 | 0.0046 ± 0.0008 | 0.982 |
| | | | Port 3 | 0.30 ± 0.07 | 1.22 ± 0.02 | 0.0076 ± 0.0007 | 0.911 |
| *R. erythropolis*-pTEC27 | **No surfactant** | ***Ex situ* measurement** | Port 1 | 0.05 ± 0.02 | 1.08 ± 0.03 | 0.031 ± 0.004 | 0.961 |
| | | | Port 2 | 0.20 ± 0.04 | 1.12 ± 0.02 | 0.019 ± 0.001 | 0.927 |
| | | | Port 3 | 0.11 ± 0.01 | 1.11 ± 0.01 | 0.013 ± 0.001 | 0.984 |
| | | **Optrode with *ex situ* sampling** | Port 1 | 0.17 ± 0.08 | 1.47 ± 0.13 | 0.1652 ± 0.0062 | 0.946 |
| | | | Port 2 | 0.11 ± 0.05 | 1.38 ± 0.04 | 0.0500 ± 0.0015 | 0.903 |
| | | | Port 3 | 0.03 ± 0.02 | 1.48 ± 0.02 | 0.0313 ± 0.0012 | 0.791 |
| | | **Optrode without *ex situ* sampling** | Port 1 | 0.14 ± 0.05 | 1.35 ± 0.04 | 0.0700 ± 0.0044 | 0.836 |
| | | | Port 2 | 0.16 ± 0.03 | 1.30 ± 0.02 | 0.0332 ± 0.0012 | 0.941 |
| | | | Port 3 | 0.10 ± 0.02 | 1.25 ± 0.01 | 0.0200 ± 0.0003 | 0.896 |
| | **Rhamnolipid** | ***Ex situ* measurement** | Port 1 | 0.25 ± 0.08 | 1.34 ± 0.06 | 0.010 ± 0.003 | 0.932 |
| | | | Port 2 | 0.24 ± 0.02 | 1.18 ± 0.08 | 0.0001 ± 0.001 | 0.990 |
| | | | Port 3 | 0.25 ± 0.03 | 1.14 ± 0.01 | 0.0001 ± 0.0003 | 0.940 |
| | | **Optrode with *ex situ* sampling** | Port 1 | 0.17 ± 0.02 | 1.79 ± 0.05 | 0.1781 ± 0.0019 | 0.993 |
| | | | Port 2 | 0.13 ± 0.03 | 1.31 ± 0.01 | 0.0525 ± 0.0004 | 0.993 |
| | | | Port 3 | 0.25 ± 0.04 | 1.59 ± 0.02 | 0.0247 ± 0.0006 | 0.936 |
| | | **Optrode without *ex situ* sampling** | Port 1 | 0.15 ± 0.07 | 1.30 ± 0.03 | 0.0380 ± 0.0028 | 0.894 |
| | | | Port 2 | 0.15 ± 0.04 | 1.24 ± 0.01 | 0.0184 ± 0.0008 | 0.946 |
| | | | Port 3 | 0.15 ± 0.02 | 1.20 ± 0.01 | 0.0089 ± 0.0003 | 0.921 |

Estimated value ± standard deviation.

ANOVA test suggested that value of the dispersion and retardation coefficients estimated using the optrode data show less variability and are more consistent among the three sampling ports ($P > 0.05$) (Table 1). These findings reveal that the optrode can efficiently perform *in situ* monitoring of bacterial transport in laboratory experiments to provide proof of concept evidence to design formulation for effective bioremediation.

### 3.3. The effect of bacterial hydrophobicity and rhamnolipid surfactant on bacterial transport behaviour in experiment 2

The effect of the hydrophobicity of bacteria and rhamnolipid addition on bacterial transport was compared using the results of experiment 2. Similar patterns were observed for all BTCs, as shown in Figs. 2–5(c). The maximum concentration of bacteria in BTCs decreased with increasing travel distance (Figs. 2–5 (c)). The CDE model performed reasonably well in describing the BTCs as the $R^2$ values ranged from 0.757 to 0.982 (Table 1). The fitted parameters showed similar patterns where the highest value of first-order decay ($\mu$) was always observed at Port 1, and values decreased with increasing travelling distance (Table 1). This finding is in agreement with a previous study (Gargiulo et al., 2008) showing that most bacterial cells were retained near the inlet and that the rate of deposition rapidly decreased with the increase in travelling distance. No significant difference was found in the

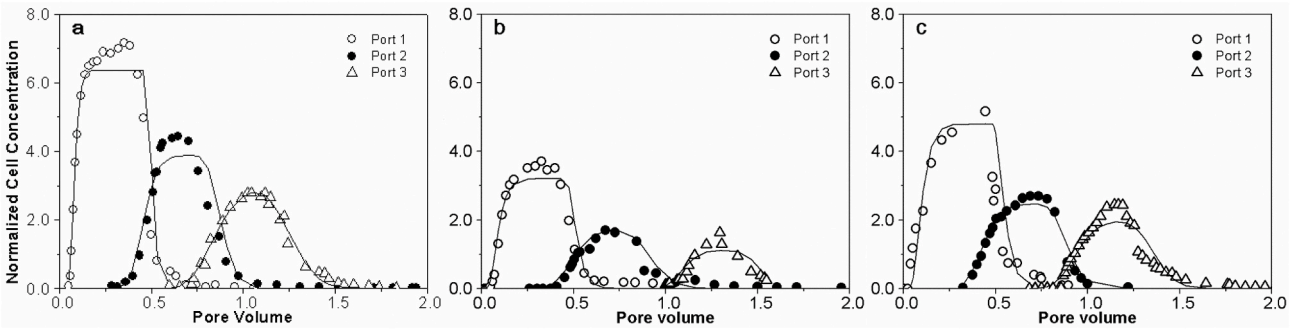


**Fig. 4.** Comparison of the observed and fitted breakthrough curves of *R. erythropolis* (pTEC27) in no surfactant obtained by *ex situ* measurements (a), the optrode in Experiment 1 (b) and the optrode in Experiment 2 (c). Symbols and lines are the same as the described in Fig. 2. Cell concentration is normalized by a normalisation factor ($1.0 \times 10^9$ CFU/mL).

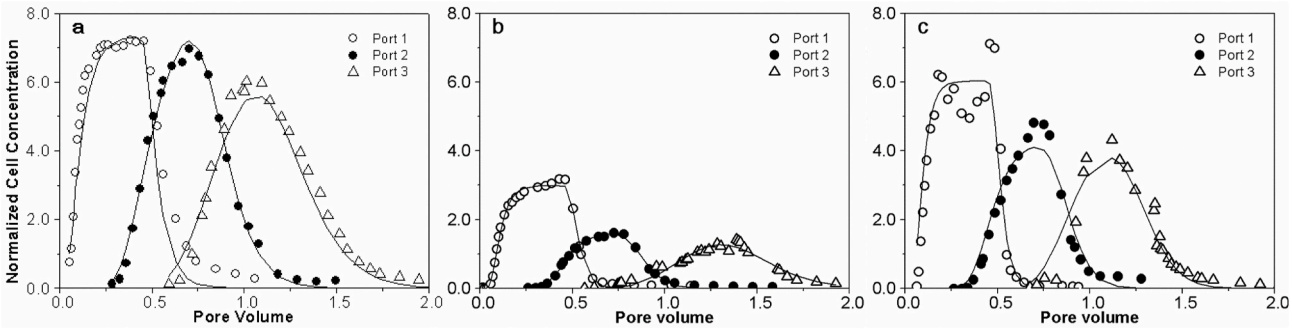


**Fig. 5.** Comparison of the observed and fitted breakthrough curves of *R. erythropolis* (pTEC27) in rhamnolipid surfactant obtained by *ex situ* measurements (a), the optrode in Experiment 1 (b) and the optrode in Experiment (c). Symbols and lines are the same as the described in Fig. 2. Cell concentration is normalized by a normalisation factor ($1.0 \times 10^9$ CFU/mL).

dispersion and retardation values between the different ports (Table 1), indicating that the column was homogeneously packed (Huang et al., 2006), which is consistent with the observation in Section 3.1.2 .

### 3.3.1. *Bacterial transport with different hydrophobicity*

The fitted transport parameter of hydrophilic *P. putida* KT2442-Gfp and hydrophobic *R. erythropolis* (pTEC27) in the absence of surfactant solution was compared to assess the effect of bacterial hydrophobicity on their transport in the column. Without the addition of rhamnolipid surfactant, the value of $\mu$ for hydrophilic *P. putida* KT2442-Gfp decreased as the increase of travelling distance (Table 1). Larger respective values of $\mu$ were observed for hydrophobic *R. erythropolis* (pTEC27) as shown in Table 1, which is consistent with previous studies that more hydrophobic bacteria have a stronger affinity to porous media during transport without surfactant solution (Chen et al., 2004; Chen and Zhu, 2005; Gargiulo et al., 2008). These observations indicate that hydrophilic *P. putida* KT2442-Gfp tends to transport faster through columns than hydrophobic *R. erythropolis* (pTEC27) does.

### 3.3.2. *The effect of rhamnolipid surfactant on bacterial transport*

Rhamnolipid surfactant was introduced to study the effect of surfactants on bacterial transport. The trends observed for the BTCs were similar in the absence and presence of rhamnolipid surfactant for both hydrophilic *P. putida* KT2442-Gfp (Figs. 2c and 3c) and hydrophobic *R. erythropolis* (pTEC27) (Figs. 4c and 5c). However, the addition of surfactant resulted in a higher peak bacterial concentration in the BTCs for both bacteria, smaller $\mu$ values and greater $D$ values for both bacteria (Table 1). Rhamnolipid surfactant did not influence $R_d$ values (Table 1). When comparing the transport behaviour of hydrophobic and hydrophilic bacteria, BTCs of hydrophilic *P. putida* KT2442-Gfp showed a greater value of $D$ and $R_d$ than that of hydrophobic *R. erythropolis* (pTEC27). While a smaller value of $\mu$ was observed for hydrophilic *P. putida* KT2442-Gfp compared to hydrophobic *R. erythropolis* (pTEC27). These findings revealed that rhamnolipid surfactant enhanced the transport of both hydrophobic and hydrophilic bacteria which is consistent with the observations of earlier studies where rhamnolipid surfactant promoted the transport of bacteria (e.g. *Lactobacillus casei*, *Streptococcus mitis* and *Pseudomonas aeruginosa* ATCC 9027, ATCC 27853, and ATCC 15442) (Bai et al., 1997; Chen et al., 2004; Zhong et al., 2016). Rhamnolipid surfactant modifies the surface tension parameters of both bacteria and sand particles by changing the contact angle (Table S1). The Lifshitz-van der Waals and the acid-base energy (*LW-AB*) interactions which are based on the surface tension parameters of bacteria and sand particles were calculated (Fig. 6). Hydrophobic bacteria have an attractive *LW-AB* interaction ($\Delta G_{bls}$) (−34.6 and −5.9 mJ/m$^2$ in the absence and presence of rhamnolipid surfactant, respectively) with sand particles (Fig. 6). While a repulsive *LW-AB* interaction ($\Delta G_{bls}$) (10.2 and 32.6 mJ/m$^2$ in the absence and presence of rhamnolipid surfactant, respectively) was calculated between hydrophilic bacteria and sand particles. The results for the *LW-AB* interaction energy support the observation that hydrophilic bacteria tend to transport more easily inside the column than hydrophobic bacteria. Rhamnolipid surfactant increased the value of the *LW-AB* interaction energy between bacteria and sand particles thereby weakening the attraction between hydrophobic *R. erythropolis* (pTEC27) and sand particles while enhancing the repulsive interaction between hydrophilic *P. putida* KT2442-Gfp and sand particles. As a consequence, enhanced bacterial transport was obtained with the addition of rhamnolipid surfactant for both bacterial strains. These results further demonstrate that the optrode can monitor the impact of bacterial hydrophobicity (e.g. hydrophilic and hydrophobic) and rhamnolipid surfactant on bacterial transport. It is expected that the *in situ* monitoring of bacterial transport under different conditions in column would be helpful for optimizing parameters of the engineering design of bioremediation applications.

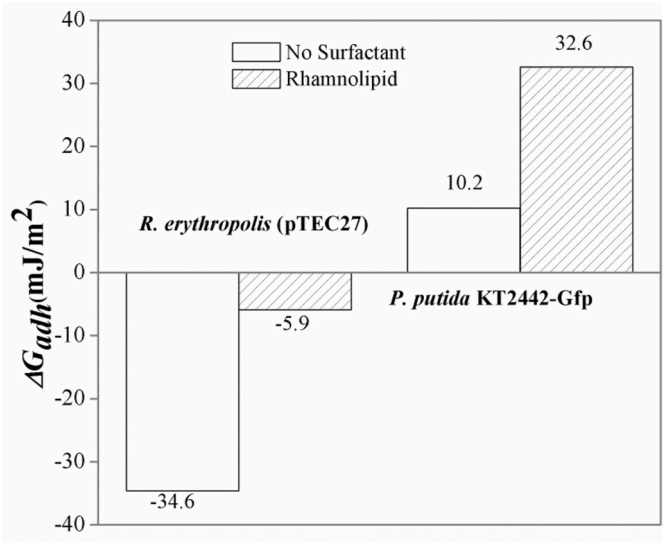


**Fig. 6.** Comparison of the calculated value of $\Delta G_{adh}$ between bacteria and sand particles.

## 4. Conclusion

The optrode provides a tool for *in situ* characterisation and monitoring of bacterial transport in a substrate environment owing to its unique advantages of allowing real-time and non-invasive detection of fluorescent bacteria. For accurate *in situ* characterisation it is important to not remove samples for *ex situ* analysis during the experiment. Using the optrode the effect of bacterial hydrophobicity and rhamnolipid surfactant on bacteria transport in sand columns was observed. In future studies, we hope to further investigate the application of the optrode in more complex column environments, e.g. columns with small flow rate, and 2D or 3D columns, to gain more in depth information on the distribution of exogenous bacteria after they are introduced for bioremediation purposes. The optrode also has great potential to become an alternative means to monitoring the transport of virus, fungi and protozoa once they are fluorescently labelled.

## Credit author statement

Wei Tao: Data curation; Formal analysis, Writing-Original draft preparation, Funding acquisition, Validation; Visualization, Investigation; Methodology Yantao Song: Writing- Reviewing and Editing, Supervision Naresh Singhal: Writing- Reviewing and Editing, Supervision Cushla McGoverin: Writing- Reviewing and Editing, Software Frédérique Vanholsbeeck: Writing- Reviewing and Editing, Software Simon swift: Writing- Reviewing and Editing; Resources; Supervision.

## Declaration of competing interest

The authors declare that they have no known competing financial interests or personal relationships that could have appeared to influence the work reported in this paper.

## Acknowledgments

This work was supported by the China Scholarship Council [grant numbers 201207000005]; Sichuan University of Science and Engineering [grant numbers 2019RC20] and The University of Auckland (New Zealand).

## Appendix A. Supplementary data

Supplementary data to this article can be found online at https://doi.org/10.1016/j.jenvman.2021.112452.

## References

Absolom, D.R., Lamberti, F.V., Policova, Z., Zingg, W., van Oss, C.J., Neumann, A., 1983. Surface thermodynamics of bacterial adhesion. Appl. Environ. Microbiol. 46 (1), 90–97.
Abu-Zreig, M., Rudra, R., Dickinson, W., 2003. Effect of application of surfactants on hydraulic properties of soils. Biosyst. Eng. 84 (3), 363–372.
Aitken, M.D., Stringfellow, W.T., Nagel, R.D., Kazunga, C., Chen, S.-H., 1998. Characteristics of phenanthrene-degrading bacteria isolated from soils contaminated with polycyclic aromatic hydrocarbons. Can. J. Microbiol. 44 (8), 743–752.
Bai, G., Brusseau, M.L., Miller, R.M., 1997. Influence of a rhamnolipid biosurfactant on the transport of bacteria through a sandy soil. Appl. Environ. Microbiol. 63 (5), 1866–1873.
Banning, N., Toze, S., Mee, B., 2002. Escherichia coli survival in groundwater and effluent measured using a combination of propidium iodide and the green fluorescent protein. J. Appl. Microbiol. 93 (1), 69–76.
Barbee, G., Brown, K., 1986. Comparison between suction and free-draninage soil solution Samplers1. Soil Sci. 141 (2), 149–154.
Beutel, S., Henkel, S., 2011. In situ sensor techniques in modern bioprocess monitoring. Appl. Microbiol. Biotechnol. 91 (6), 1493–1505.
Brown, D.G., Jaffé, P.R., 2001. Effects of nonionic surfactants on bacterial transport through porous media. Environ. Sci. Technol. 35 (19), 3877–3883.
Busscher, H., Weerkamp, A., Van der Mei, H., Van Pelt, A., De Jong, H., Arends, J., 1984. Measurement of the surface free energy of bacterial cell surfaces and its relevance for adhesion. Appl. Environ. Microbiol. 48 (5), 980–983.
Campbell, C.G., Ghodrati, M., Garrido, F., 1999. Comparison of time domain reflectometry, fiber optic mini-probes, and solution samplers for real time measurement of solute transport in soil. Soil Sci. 164 (3), 156–170.
Chen, G., Qiao, M., Zhang, H., Zhu, H., 2004. Bacterial desorption in water-saturated porous media in the presence of rhamnolipid biosurfactant. Res. Microbiol. 155 (8), 655–661.
Chen, G., Strevett, K.A., 2001. Impact of surface thermodynamics on bacterial transport. Environ. Microbiol. 3 (4), 237–245.
Chen, G., Zhu, H., 2004. Bacterial deposition in porous medium as impacted by solution chemistry. Res. Microbiol. 155 (6), 467–474.
Chen, G., Zhu, H., 2005. Bacterial adhesion to silica sand as related to Gibbs energy variations. Colloids Surf. B Biointerfaces 44 (1), 41–48.
Clifford, J.S., Ioannidis, M.A., Legge, R.L., 2007. Enhanced aqueous solubilization of tetrachloroethylene by a rhamnolipid biosurfactant. J. Colloid Interface Sci. 305 (2), 361–365.
de Lorenzo, V., Eltis, L., Kessler, B., Timmis, K.N., 1993. Analysis of Pseudomonas gene products using lacIq/Ptrp-lac plasmids and transposons that confer conditional phenotypes. Gene 123 (1), 17–24.
Dennis, J.J., Zylstra, G.J., 2004. Complete sequence and genetic organization of pDTG1, the 83 kilobase naphthalene degradation plasmid from Pseudomonas putida strain NCIB 9816-4. J. Mol. Biol. 341 (3), 753–768.
Di Bonito, M., Breward, N., Crout, N., Smith, B., Young, S.D., Zhang, H., 2018. Chapter 10 - extraction and characterization of pore water in contaminated soils. In: De Vivo, B., Belkin, H.E., Lima, A. (Eds.), Environmental Geochemistry, second ed. Elsevier, pp. 195–235.
Dorn, J.G., Brusseau, M.L., Maier, R.M., 2005. Real-time, in situ monitoring of bioactive zone dynamics in heterogeneous systems. Environ. Sci. Technol. 39 (22), 8898–8905.
Feng, W., Swift, S., Singhal, N., 2013. Effects of surfactants on cell surface tension parameters and hydrophobicity of Pseudomonas putida 852 and Rhodococcus erythropolis 3586. Colloids Surf. B Biointerfaces 105, 43–50.
Gargiulo, G., Bradford, S., Simunek, J., Ustohal, P., Vereecken, H., Klumpp, E., 2008. Bacteria transport and deposition under unsaturated flow conditions: the role of water content and bacteria surface hydrophobicity. Vadose Zone J. 7 (2), 406–419.
Goude, R., Parish, T., 2009. Electroporation of Mycobacteria *Mycobacteria Protocols*. Springer, pp. 203–215.
Gross, M.J., Logan, B.E., 1995. Influence of different chemical treatments on transport of Alcaligenes paradoxus in porous media. Appl. Environ. Microbiol. 61 (5), 1750–1756.
Guo, R., McGoverin, C., Swift, S., Vanholsbeeck, F., 2017. A rapid and low-cost estimation of bacteria counts in solution using fluorescence spectroscopy. Anal. Bioanal. Chem. 409 (16), 3959–3967.
Guo, S., Liu, X., Zhao, H., Wang, L., Tang, J., 2021. High pyrolysis temperature biochar reduced the transport of petroleum degradation bacteria Corynebacterium variabile HRJ4 in porous media. J. Environ. Sci. 100, 228–239.
He, L., Wu, D., Tong, M., 2019. The influence of different charged poly (amido amine) dendrimer on the transport and deposition of bacteria in porous media. Water Res. 161, 364–371.
Heitzer, A., Malachowsky, K., Thonnard, J.E., Bienkowski, P.R., White, D.C., Sayler, G.S., 1994. Optical biosensor for environmental on-line monitoring of naphthalene and salicylate bioavailability with an immobilized bioluminescent catabolic reporter bacterium. Appl. Environ. Microbiol. 60 (5), 1487–1494.
Hewitt, B.M., Singhal, N., Elliot, R.G., Chen, A.Y., Kuo, J.Y., Vanholsbeeck, F.d. r., Swift, S., 2012. Novel fiber optic detection method for in situ analysis of

fluorescently labeled biosensor organisms. Environ. Sci. Technol. 46 (10), 5414–5421.
Huang, G., Huang, Q., Zhan, H., 2006. Evidence of one-dimensional scale-dependent fractional advection–dispersion. J. Contam. Hydrol. 85 (1), 53–71.
Huysman, F., Verstraete, W., 1993. Water-facilitated transport of bacteria in unsaturated soil columns: influence of cell surface hydrophobicity and soil properties. Soil Biol. Biochem. 25 (1), 83–90.
Lambertsen, L., Sternberg, C., Molin, S., 2004. Mini-Tn7 transposons for site-specific tagging of bacteria with fluorescent proteins. Environ. Microbiol. 6 (7), 726–732.
Lang, F.S., Destain, J., Delvigne, F., Druart, P., Ongena, M., Thonart, P., 2016. Biodegradation of polycyclic aromatic hydrocarbons in mangrove sediments under different strategies: natural attenuation, biostimulation, and bioaugmentation with Rhodococcus erythropolis T902. 1. Water,Air, Soil Pollut. 227 (9), 297.
Li, Q., Logan, B.E., 1999. Enhancing bacterial transport for bioaugmentation of aquifers using low ionic strength solutions and surfactants. Water Res. 33 (4), 1090–1100.
Maraha, N., Backman, A., Jansson, J.K., 2004. Monitoring physiological status of GFP-tagged Pseudomonas fluorescens SBW25 under different nutrient conditions and in soil by flow cytometry. FEMS (Fed. Eur. Microbiol. Soc.) Microbiol. Ecol. 51 (1), 123–132.
Martin, M.J., Logan, B.E., Johnson, W.P., Jewett, D.G., Arnold, R.G., 1996. Scaling bacterial filtration rates in different sized porous media. J. Environ. Eng. 122 (5), 407–415.
McNaught, A.D., Wilkinson, A., 1997. IUPAC. Compendium of Chemical Terminology. In: The "Gold Book"), second ed. Blackwell Scientific Publications, Oxford.
Mohan, S.V., Kisa, T., Ohkuma, T., Kanaly, R.A., Shimizu, Y., 2006. Bioremediation technologies for treatment of PAH-contaminated soil and strategies to enhance process efficiency. Rev. Environ. Sci. Biotechnol. 5 (4), 347–374.
Parker, J., Van Genuchten, M.T., 1984. Determining transport parameters from laboratory and field tracer experiments. Bulletin/Virginia Agricultural Experiment Station (USA). no, 84-3.
Sharma, P., Hanumantha Rao, K., 2002. Analysis of different approaches for evaluation of surface energy of microbial cells by contact angle goniometry. Adv. Colloid Interface Sci. 98 (3), 341–463.
Tai, D.C., Hooks, D.A., Harvey, J.D., Smaill, B.H., Soeller, C., 2007. Illumination and fluorescence collection volumes for fiber optic probes in tissue. J. Biomed. Opt. 12 (3), 034033.
Takaki, K., Davis, J.M., Winglee, K., Ramakrishnan, L., 2013. Evaluation of the pathogenesis and treatment of Mycobacterium marinum infection in zebrafish. Nat. Protoc. 8 (6), 1114.
Toride, N., Leij, F., Van Genuchten, M.T., 1995. The CXTFIT Code for Estimating Transport Parameters from Laboratory or Field Tracer Experiments, vol. 2. version.
Trzesicka-Mlynarz, D., Ward, O., 1995. Degradation of polycyclic aromatic hydrocarbons (PAHs) by a mixed culture and its component pure cultures, obtained from PAH-contaminated soil. Can. J. Microbiol. 41 (6), 470–476.
Unc, A., Goss, M.J., 2003. Movement of faecal bacteria through the vadose zone. Water, Air, Soil Pollut. 149 (1), 327–337.
Van Genuchten, M.T., Alves, W., 1982. Analytical solutions of the one-dimensional convective-dispersive solute transport equation. Tech. Bull. 1661, 2–3.
Van Oss, C., 1995. Hydrophobicity of biosurfaces—origin, quantitative determination and interaction energies. Colloids Surf. B Biointerfaces 5 (3), 91–110.
Yolcubal, I., Piatt, J.J., Pierce, S.A., Brusseau, M.L., Maier, R.M., 2000. Fiber optic detection of in situ lux reporter gene activity in porous media: system design and performance. Anal. Chim. Acta 422 (2), 121–130.
Zhang, C., Parrello, D., Brown, P.J.B., Wall, J.D., Hu, Z., 2018. A novel whole-cell biosensor of Pseudomonas aeruginosa to monitor the expression of quorum sensing genes. Appl. Microbiol. Biotechnol. 102 (14), 6023–6038.
Zhang, Y., Maier, W.J., Miller, R.M., 1997. Effect of rhamnolipids on the dissolution, bioavailability, and biodegradation of phenanthrene. Environ. Sci. Technol. 31 (8), 2211–2217.
Zhang, Y., Miller, R.M., 1994. Effect of a Pseudomonas rhamnolipid biosurfactant on cell hydrophobicity and biodegradation of octadecane. Appl. Environ. Microbiol. 60 (6), 2101–2106.
Zhao, Z., Selvam, A., Wong, J.W.-C., 2011. Effects of rhamnolipids on cell surface hydrophobicity of PAH degrading bacteria and the biodegradation of phenanthrene. Bioresour. Technol. 102 (5), 3999–4007.
Zhong, H., Liu, G., Jiang, Y., Brusseau, M.L., Liu, Z., Liu, Y., Zeng, G., 2016. Effect of low-concentration rhamnolipid on transport of Pseudomonas aeruginosa ATCC 9027 in an ideal porous medium with hydrophilic or hydrophobic surfaces. Colloids Surf. B Biointerfaces 139, 244–248.